Lineal-path function for random heterogeneous materials

Binglin Lu
Department of Mechanical and Aerospace Engineering, North Carolina State University, Raleigh, North Carolina 27695-7910

S. Torquato
Department of Mechanical and Aerospace Engineering
and Department of Chemical Engineering, North Carolina State University, Raleigh, North Carolina 27695-7910
(Received 16 September 1991)

A fundamental morphological measure of two-phase heterogenous materials is what we refer to as the lineal-path function $L(z)$. This quantity gives the probability that a line segment of length z is wholly in one of the phases, say phase 1, when randomly thrown into the sample. For three-dimensional systems, we observe that $L(z)$ is also equivalent to the area fraction of phase 1 measured from the projected image onto a plane: a problem of long-standing interest in stereology. We develop a theoretical means of representing and computing the lineal-path function $L(z)$ for distributions of D-dimensional spheres with arbitrary degree of penetrability using statistical-mechanical concepts. In order to test our theoretical results, we determined $L(z)$ from Monte Carlo simulations for the case of three-dimensional systems of spheres and found very good agreement between theory and the Monte Carlo calculations.

PACS number(s): 47.55.Mh, 05.20.−y, 61.20.Gy

I. INTRODUCTION

A fundamental understanding of the effective transport, electromagnetic, and mechanical properties of random heterogeneous materials, such as porous media and composite materials, rests on the ability to quantitatively characterize the microstructure of the media. Indeed, complete characterization of the microstructure requires knowledge of an infinite set of statistical correlation functions [1]. In practice, only lower-order information is obtainable either experimentally or theoretically. The problem of ascertaining whether there exist lower-order functions that simultaneously contain significant microstructural information remains an important line of research.

It is instructive to briefly review the various types of lower-order functions that have been previously investigated for two-phase media [1]. The most basic and simplest quantity is the *volume fraction of phase i*, ϕ_i. This is actually a one-point correlation function, since it is equivalent, in the case of a statistically homogeneous system, to the probability of finding a point in phase i. Another important one-point correlation function is the *specific surface* s, the interfacial surface area per unit volume.

The two-point probability function $S_2^{(i)}(\mathbf{x}_1,\mathbf{x}_2)$ gives the probability of finding two points at positions $\mathbf{x}_1$ and $\mathbf{x}_2$ in phase i. The quantity $S_2^{(i)}(r)-\phi_i^2$ for an isotropic system ($r\equiv|\mathbf{x}_2-\mathbf{x}_1|$) equals the constant $\phi_i-\phi_i^2$ at $r=0$ and equals zero for $r\to\infty$, assuming no long-range order. For intermediate values of r, $S_2^{(i)}(r)-\phi_i^2$ may take on positive as well as negative values, giving a rough measure of the characteristic lengths of phase i. Indeed, a characteristic length of phase i may be defined as

$$l_i=\int_0^\infty [S_2^{(i)}(r)-\phi_i^2]dr \ . \tag{1.1}$$

However, since $S_2^{(1)}-\phi_1^2=S_2^{(2)}-\phi_2^2$, the two-point probability function cannot distinguish between phase-1 and phase-2 materials. [More generally, the n-point function $S_n(\mathbf{x}_1,\ldots,\mathbf{x}_n)$ gives the probability of finding n points at $\mathbf{x}_1,\ldots,\mathbf{x}_n$ all in phase 1, and is fundamental to the study of the conductivity [2], elastic moduli [3], trapping rate [4,5] and fluid permeability [4,6,7] of heterogeneous media.] The two-point surface-void function $F_{SV}(\mathbf{x}_1,\mathbf{x}_2)$ and surface-surface function $F_{SS}(\mathbf{x}_1,\mathbf{x}_2)$ arise in rigorous bounds on the trapping rate among static traps [4,5] and the fluid permeability [4,7]. Another two-point function of basic importance for porous materials is the so-called *pore-size distribution* $P(\delta)$. The quantity $P(\delta)d\delta$ gives the probability that a point in the pore phase (say phase 1) lies at a distance between δ and $\delta+d\delta$ from the nearest point on the pore-solid interface. A characteristic pore size can be defined as

$$l_P=\int_0^\infty \delta P(\delta)d\delta \ . \tag{1.2}$$

The length l_P is a more accurate measure of the characteristic length of phase 1, the pore phase, than the length l_i defined by (1.1). The pore-size distribution naturally arises in diffusion and reaction in heterogeneous media [8].

All of the statistical correlation functions described above are actually special cases of the general n-point distribution function H_n introduced by Torquato [9]. For the case of heterogeneous media composed of identical spheres of arbitrary penetrability, he derived exact series representations of H_n in terms of the n-particle distribution functions: quantities which are, in principle, known for the given statistical ensemble. Lu and Torquato [10] subsequently generalized this formalism to obtain H_n for sphere distributions with a polydispersivity in size.

The formation of very large "clusters" in particle sys-

tems can have a dramatic influence on the macroscopic properties of the media. A cluster of phase i is defined as that part of phase i which can be reached from a point in phase i without passing through phase $j \neq i$. Unfortunately, *lower-order* H_n do not reflect information about large clusters in the system. Torquato, Beasley, and Chiew [11] have introduced and represented the so-called two-point cluster function $C_2^{(i)}(\mathbf{x}_1,\mathbf{x}_2)$ defined to be the probability of finding two points at x_1 and x_2 in the same cluster of phase i or, equivalently, the probability that a point can move along a *lineal path* of length z in phase i without passing through the other phase. Thus, $C_2^{(i)}$ is the analog of $S_2^{(i)}$ but, unlike its predecessor, contains topological "connectedness" information. The measurement of $C_2^{(i)}$ for real material samples is nontrivial since it cannot be obtained from a two-dimensional cross section of the material, i.e., it is an intrinsically three-dimensional measurement.

Another interesting and useful statistical measure is what we shall refer to as the "lineal-path function" $L^{(i)}(z)$. This quantity is the probability that a line segment of length z is wholly in phase i. For three-dimensional systems, we observe that $L^{(i)}(z)$ is actually also equivalent to the area fraction of phase i measured from the projected image of a three-dimensional slice of thickness z onto a plane. Figure 1 depicts the projection of a two-dimensional particle system onto a line. It is a problem of long-standing interest in stereology to evaluate the projected area fraction or, equivalently, the lineal-path function $L^{(i)}(z)$ for three-dimensional particle systems. Its evaluation for nondilute particle concentrations remains a challenging theoretical problem because of, in the language of Underwood [12], "overlap" effects due to projection of the three-dimensional image and "truncation" effects due to slicing the system (see Fig. 1). To our knowledge, the lineal-path function has yet to be computed for many-particle systems at nondilute concentrations.

The purpose of this paper is to develop a means of representing and calculating the lineal-path function $L(z) \equiv L^{(1)}(z)$ for general distributions of spheres (phase 2) using statistical-mechanical concepts. In light of our observation, this quantity also yields the projected area fraction for such models. In a future paper we shall discuss the implications of knowledge of the lineal-path function for transport in porous media [13].

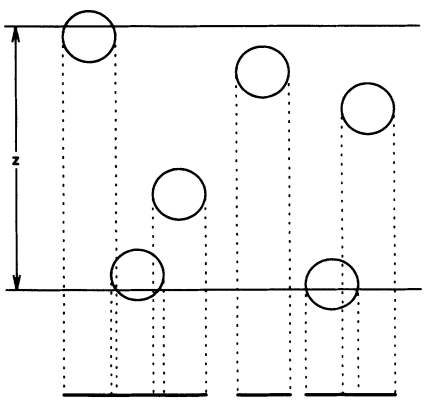

FIG. 1. The projection of a two-dimensional system of spheres onto a line. Note that z is the thickness of the slice. The heavy solid line represents the projected image of the particles.

In Sec. II we develop an exact series representation of the lineal-path function $L(z)$ for systems of D-dimensional, identical, possibly penetrable spheres. In the case of fully penetrable spheres, we obtain $L(z)$ exactly for arbitrary dimensionality. In Sec. III we derive approximate but accurate expressions of $L(z)$ for the instance of hard spheres for $D=1$, 2, and 3. We also perform Monte Carlo calculations of $L(z)$ for the case $D=3$ and find very good agreement between theory and Monte Carlo data.

II. EXACT REPRESENTATION OF THE LINEAL PATH FUNCTION $L(z)$ FOR RANDOM ARRAYS OF IDENTICAL SPHERES

A. System description and general n-point distribution function H_n

We consider a system of N identical, interacting D-dimensional spheres of radius R spatially distributed in a volume V according to the N-particle probability density $P_N(\mathbf{r}^N)$. The specific probability density $P_N(\mathbf{r}^N)$ characterizes the probability of finding the particles labeled $1,2,\ldots,N$ with configuration $\mathbf{r}^N \equiv \{\mathbf{r}_1,\mathbf{r}_2,\ldots,\mathbf{r}_N\}$, respectively, and normalizes to unity. The reduced n-particle generic probability density ρ_n $(n<N)$ is defined by

$$\rho_n(\mathbf{r}^n)=\frac{N!}{(N-n)!}\int P_N(\mathbf{r}^N)d\mathbf{r}^{N-n}\,, \tag{2.1}$$

where $d\mathbf{r}^{N-n} \equiv d\mathbf{r}_{n+1}\cdots d\mathbf{r}_N$. Thus, $\rho_n(\mathbf{r}^n)$ characterizes the probability of simultaneously finding the center of a particle in volume element $d\mathbf{r}_1$ about $\mathbf{r}_1$, the center of another particle in volume element $d\mathbf{r}_2$ about $\mathbf{r}_2$, etc. The ensemble average of any many-body function $F(\mathbf{r}^N)$ is given by

$$\langle F(\mathbf{r}^N)\rangle = \int F(\mathbf{r}^N)P_N(\mathbf{r}^N)d\mathbf{r}^N\,. \tag{2.2}$$

If the medium is statistically homogeneous, the $\rho_n(\mathbf{r}^n)$ depend upon the relative displacements $\mathbf{r}_2-\mathbf{r}_1$, $\mathbf{r}_3-\mathbf{r}_1,\ldots,\mathbf{r}_n-\mathbf{r}_1$. In such instances, it is implied that the "thermodynamic limit" has been taken, i.e., $N\to\infty$, $V\to\infty$, such that $\rho=N/V=\rho_1(\mathbf{r}_1)$ is some finite constant.

Torquato [9] has introduced the general n-point distribution function $H_n(\mathbf{x}^m;\mathbf{x}^{p-m};\mathbf{r}^q)$ which is defined to be the correlation associated with finding m points with positions $\mathbf{x}^m \equiv \{\mathbf{x}_1,\ldots,\mathbf{x}_m\}$ on certain surfaces in the system, $p-m$ points with positions $\mathbf{x}^{p-m} \equiv \{\mathbf{x}_{m+1},\ldots,\mathbf{x}_p\}$ in certain regions exterior to the spheres, and any q of the spheres with configuration $\mathbf{r}^q$, where $n=p+q$, in a statistically *inhomogeneous* medium of N identical D-dimensional interpenetrable spheres. He found two different series representations of H_n for such media in terms of the $\rho_n(\mathbf{r}^n)$ that enable one to compute it. The

key idea in arriving at these representations is the "available space" to "test" particles which are added to the system of N spherical inclusions of radius R. Consider adding p test particles of radius $b_1, \ldots, b_p$, $p \ll N$. Since the ith test particle is capable of excluding the centers of the actual inclusions from spheres of radius a_i (where for $b_i > 0$, $a_i = R + b_i$), then it is natural to associate with each test particle a subdivision of space into two regions: D_i, the space available to the ith test particle, and D_i^*, the space unavailable to the ith test particle. Let S_i denote the surface between D_i and D_i^*. Then, more specifically, $H_n(\mathbf{x}^m;\mathbf{x}^{p-m};\mathbf{r}^q)$ gives the correlation associated with finding the test particle of radius b_1 at $\mathbf{x}_1$ on $S_1, \ldots,$ the test particle of radius b_m at $\mathbf{x}_m$ on S_m, the test particle of radius b_{m+1} at $\mathbf{x}_{m+1}$ in $D_{m+1}, \ldots,$ and the test particle of radius b_p at $\mathbf{x}_p$ in D_p, and of finding any q inclusions with configuration $\mathbf{r}^q$. Note that it is only in the limit $a_i \to R$ that D_i is the space exterior to the actual inclusions, i.e., the matrix or void phase.

From the general quantity H_n, one can obtain all of the different types of correlation functions (described in the Introduction) that have arisen in rigorous expressions for effective properties of random arrays of spheres. For example, one has

$$S_n(\mathbf{x}_n) \equiv S_n^{(1)}(\mathbf{x}_n) = \lim_{a_i \to R(\forall_i)} H_n(0;\mathbf{x}^n;0) , \tag{2.3}$$

$$F_{SS}(\mathbf{x}_1,\mathbf{x}_2) = \lim_{a_i \to R(\forall_i)} H_2(\mathbf{x}_1,\mathbf{x}_2;0;0) , \tag{2.4}$$

$$H_V(r) = H_1(\mathbf{x}_1;0;0), \quad (b_1 = r - R) , \tag{2.5}$$

$$E_V(r) = H_1(0;\mathbf{x}_1;0), \quad (b_1 = r - R)$$
$$= 1 - \int_0^r H_V(r)dr . \tag{2.6}$$

The quantity $H_V(r)$ is the "void" nearest-neighbor distribution described by Torquato, Lu, and Rubinstein [14] and is equal to $\phi_1 P(r)$, where ϕ_1 is the volume fraction of the void phase and $P(r)$ is the pore size distribution as defined in the Introduction. The quantity $E_V(r)$ is the void exclusion probability and gives the probability of finding a region Ω_E, which is a spherical cavity of radius $r = b_1 + R$ centered at some arbitrary point, empty of inclusion centers. Both H_V and E_V are actually *two-point* correlation functions because the test particle has non zero radius. We shall show below that the lineal-path function $L(z)$ is actually a special type of exclusion probability function.

B. Calculation of the exclusion probability function

For the case of D-dimensional fully penetrable spherical inclusions, i.e., spatially uncorrelated spheres,

$$\rho_n(\mathbf{r}^n) = \rho^n , \tag{2.7}$$

exactly, and the exact series representation of $E_V(r)$ yields the simple expression

$$E_V(x) = \exp\left[-\eta \frac{v_D(x)}{v_D(1)}\right] , \tag{2.8}$$

where

$$v_3(x) = \frac{\pi x^3}{6} , \tag{2.9}$$

$$v_2(x) = \frac{\pi x^2}{4} , \tag{2.10}$$

$$v_1(x) = x , \tag{2.11}$$

$$x = \frac{r}{2R} , \tag{2.12}$$

and

$$\eta = \rho v_D(1) \tag{2.13}$$

is a reduced density. In the instance of totally impenetrable or hard spheres, the exact series representation of $E_V(r)$ can only be evaluated exactly for the case $D = 1$ (i.e., hard rods) [14]. It is impossible to evaluate $E_V(r)$ for $D \geq 2$ because the n-particle probability densities $\rho_n(\mathbf{r}^n)$ are not known exactly. One must therefore devise approximate schemes to evaluate and sum the series. Torquato, Lu, and Rubinstein [14] obtained $E_V(r)$ from the Percus-Yevick [15], scaled-particle [16,17], and Carnahan-Starling [18] approximations for the related conditional "pair" distribution function $G_V(r)$ (described in Sec. III). For example, the scaled-particle result for the exclusion probability for $D = 3$ is given by

$$E_V(x) = \begin{cases} 1 - 8\eta x^3, & 0 \leq x \leq \frac{1}{2} \\ (1-\eta)\exp[-\eta(8ax^3 + 12bx^2 + 24cx + d)], & x > \frac{1}{2} \end{cases} \tag{2.14}$$

where

$$a(\eta) = \frac{1 + \eta + \eta^2}{(1-\eta)^3} , \tag{2.15}$$

$$b(\eta) = \frac{-3\eta(1+\eta)}{2(1-\eta)^3} , \tag{2.16}$$

$$c(\eta) = \frac{3\eta^2}{4(1-\eta)^3} , \tag{2.17}$$

$$d(\eta) = \frac{-11\eta^2 + 7\eta - 2}{2(1-\eta)^3} , \tag{2.18}$$

where the dimensionless distance is given by (2.12) and η is given by (2.13) with $D = 3$.

For hard disks ($D = 2$), the corresponding scaled-particle expression for the exclusion probability function is

$$E_V(x) = \begin{cases} 1 - 4\eta x^2, & 0 \leq x \leq \frac{1}{2} \\ (1-\eta)\exp\left[\dfrac{-\eta(4x^2 - 4\eta x + 2\eta - 1)}{(1-\eta)^2}\right], & x > \frac{1}{2} \end{cases} \tag{2.19}$$

where η is given by (2.13) with $D = 2$.

It is only in the case of one-dimensional hard rods of length $2R$ that the exclusion probability function is known exactly for D-dimensional hard spheres.

Specifically, one has

$$E_V(x)=\begin{cases}1-2\eta x, & 0\le x\le\frac{1}{2}\\ (1-\eta)\exp\left[\dfrac{-2\eta(x-\frac{1}{2})}{1-\eta}\right], & x>\frac{1}{2}\end{cases} \tag{2.20}$$

where η is given by (2.13) with $D=1$.

C. Series representation of lineal-path function

The derivation of the exact series representation of the lineal-path function $L(z)$ follows closely the derivation of the corresponding expression for the exclusion probability function $E_V(r)$ for a spherical test particle of radius $b_1=r-R$. This is done by recognizing that $L(z)$ is a special type of exclusion probability function, i.e., the probability of inserting a test particle which is a line of length z into the system is equal to the probability of finding a region $\Omega_E(z)$, which is the exclusion region between a line of length z and a sphere of radius R, empty of inclusion centers. The region $\Omega_E(z)$ in this case is therefore a D-dimensional spherocylinder of cylindrical length z and radius R with hemispherical caps of radius R on either end (see Fig. 2). Following Torquato [9], then we introduce the exclusion region indicator function

$$m(\mathbf{y};z)=\begin{cases}1, & \mathbf{y}\in\Omega_E(z)\\ 0, & \text{otherwise},\end{cases} \tag{2.21}$$

where $\mathbf{y}$ is measured from the centroid.

Given the result (2.16), then the derivation of the series representation of $L(z)$ follows in exactly the same fashion as that for spherical test particles and hence we find

$$L(z)=1+\sum_{k=1}^{\infty}\frac{(-1)^k}{k!}\int\rho_k(\mathbf{r}^k)\prod_{j=1}^{k}m_j(\mathbf{x}-\mathbf{r}_j;z)d\mathbf{r}_j\ . \tag{2.22}$$

In the instance of fully penetrable spherical inclusions, results (2.7) and (2.22) yield the exact result

$$L(z)=\exp[-\rho v_E(z)]\ , \tag{2.23}$$

where $v_E(z)$ is the D-dimensional volume of the exclusion region Ω_E,

$$v_E=\frac{4\pi}{3}R^3+\pi R^2 z\quad (D=3)\ , \tag{2.24}$$

$$v_E=\pi R^2+2Rz\quad (D=2)\ , \tag{2.25}$$

$$v_E=2R+z\quad (D=1)\ . \tag{2.26}$$

Since the porosity ϕ_1 (i.e., the volume fraction of the space exterior to the spheres) for fully penetrable sphere is simply given by

$$\phi_1=\exp(-\eta)\ , \tag{2.27}$$

where η is given by (2.13), then the lineal-path function

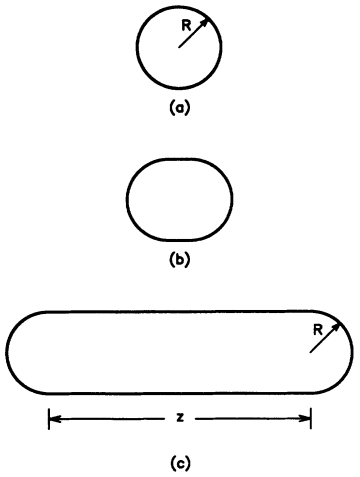

FIG. 2. (a) Spherical cavity of radius R; (b) expansion of a spherical cavity into a spherocylinder; (c) final spherocylinder with cylindrical length z and radius R with hemispherical caps of the same radius.

may be written as

$$L(x)=\phi_1^{1+(3/2)x}\quad (D=3)\ , \tag{2.28}$$

$$L(x)=\phi_1^{1+(4/\pi)x}\quad (D=2)\ , \tag{2.29}$$

$$L(x)=\phi_1^{1+x}\quad (D=1)\ , \tag{2.30}$$

where $x=z/2R$ is a dimensionless distance. These new analytical results are displayed in Fig. 3. For any D, $L(x)$ is a monotonic decreasing function of x. This behavior is expected since the larger the line segment or "slice" of material of length x is, the smaller is the probability of finding the line wholly in the matrix or the smaller is the "projected area." For fixed x, $L(x)$ decreases

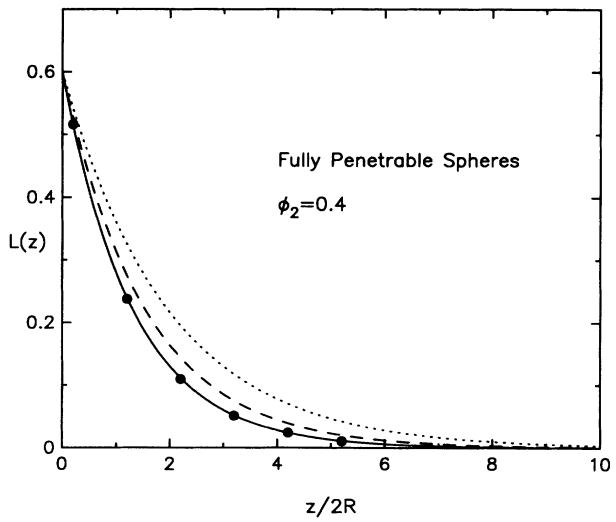

FIG. 3. Lineal-path function $L(z)$ vs the dimensionless distance $z/2R$ for D-dimensional fully penetrable spheres at a sphere volume fraction $\phi_2=0.4$, as obtained from (2.28)–(2.30). The solid line is for $D=3$, the dashed line is for $D=2$, and the dotted line is for $D=1$. The solid circles are our Monte Carlo simulation results for $D=3$.

with increasing dimensionality because the spheres fill space more efficiently as D increases. In the case of three dimensions, we performed Monte Carlo calculations of $L(z)$ (see Appendix A for details). It is seen that the Monte Carlo evaluations are in excellent agreement with the exact analytical results, validating the accuracy of the simulation method which is also used to compute $L(z)$ for hard-sphere systems.

For impenetrable spherical inclusions, an exact evaluation of the series (2.22) is out of the question for the same reasons given earlier. The subsequent section describes the derivation of an approximate but accurate expression for $L(z)$ for hard-sphere systems.

III. ANALYTICAL EXPRESSIONS FOR THE LINEAL-PATH FUNCTION FOR D-DIMENSIONAL HARD SPHERES

We assume that the system of D-dimensional hard spheres is in thermal equilibrium. This enables us to exploit the well-established concepts of equilibrium statistical mechanics to obtain approximate but accurate expressions for the lineal-path function $L(z)$ for such models. We specifically use the fact that the reversible work $W(z,R)$ required for the creation of D-dimensional spherocylindrical *cavity* (of cylindrical length z and radius R, capped at each end by a hemisphere of the same radius) in a D-dimensional hard-sphere system is exactly related to the probability of finding this cavity empty of sphere centers, $L(z)$, by

$$L(z)=\exp\left[\frac{-W(z,R)}{kT}\right], \tag{3.1}$$

where k is the Boltzmann constant and T is the temperature of the system. Since the reversible work done to create the cavity is process independent, then we can consider the simplest process to calculate W. First we create a spherical cavity of radius R. Let the work done for this part be denoted by W_1. Then we expand the spherical cavity along one direction to create a spherocylinder (see Fig. 2). Let W_2 denote the work for this expansion process. Therefore,

$$W(z,R)=W_1(R)+W_2(z,R) . \tag{3.2}$$

The work $W_1(R)$ is related to the exclusion probability $E_V(x)$ evaluated at $x=r/2R=\frac{1}{2}$ by

$$W_1(R)=-kT\ln E_V(x=\tfrac{1}{2}) , \tag{3.3}$$

and therefore

$$L(z)=E_V(x=\tfrac{1}{2})\exp\left[-\frac{W_2(z,R)}{kT}\right]$$
$$=\phi_1\exp\left[-\frac{W_2(z,R)}{kT}\right] . \tag{3.4}$$

The simplest way of calculating $L(z)$ is to obtain W_2 from the initial infinitesimal expansion process, i.e., from a sphere of radius R to a spherocylinder of length dz and radius R.

The work $W_2(z,R)$ needed to expand the spherical cavity into a spherocylinder is itself composed of two parts: the work needed to overcome the pressure W_P and the work needed to overcome the surface tension W_S,

$$W_2(z,R)=W_P(z,R)+W_S(z,R) . \tag{3.5}$$

In the thermodynamic limit, the pressure does not change as the cavity expands into a spherocylinder. Therefore, we have

$$W_P=p\Delta V , \tag{3.6}$$

where ΔV is the change in volume for the expansion process

$$\Delta V=\pi R^2 z \quad (D=3) , \tag{3.7}$$

$$\Delta V=2Rz \quad (D=2) , \tag{3.8}$$

$$\Delta V=z \quad (D=1) . \tag{3.9}$$

Accurate equations of state for D-dimensional hard spheres are given by

$$\frac{p}{\rho kT}=\frac{1+\eta+\eta^2}{(1-\eta)^3} \quad (D=3) , \tag{3.10}$$

$$\frac{p}{\rho kT}=\frac{1}{(1-\eta)^2} \quad (D=2) , \tag{3.11}$$

$$\frac{p}{\rho kT}=\frac{1}{1-\eta} \quad (D=1) . \tag{3.12}$$

Relations (3.10) and (3.11) are the scaled-particle approximations for the pressure. For $D=3$, relation (3.10) is the same as predicted by the Percus-Yevick approximation. The one-dimensional result (3.12) is exact.

The work associated with surface change can be obtained through the relation

$$dW_S=\sigma dS . \tag{3.13}$$

Following Reiss, Frisch, and Lebowitz [16], we take the surface tension of the cavity with arbitrary local radius of curvature ξ to be given by

$$\sigma=\sigma_0\left[1-\frac{\delta}{\xi}\right] , \tag{3.14}$$

where σ_0 and δ are density-dependent parameters which are to be determined from the void conditional pair-distribution function $G_V(r)$. The quantity $\rho s_D(r)G_V(r)dr$ is the probability, given a spherical cavity of radius r is empty of sphere centers, that particle centers are contained in the spherical shell of volume $s_D(r)dr$ encompassing the cavity. Here $s_D(r)$ is the surface area of a D-dimensional sphere of radius r,

$$s_3(r)=4\pi r^2 , \tag{3.15}$$

$$s_2(r)=2\pi r , \tag{3.16}$$

$$s_1(r)=2 . \tag{3.17}$$

As noted earlier, we compute the surface tension contri-

bution to the work W_S from the initial infinitesimal expansion process. Therefore, the local radius of curvature ξ is R, and hence the surface tension for the expansion process is equal to that for a spherical cavity of radius R. Now since $E_V(r)$ and $G_V(r)$ are related by the formula

$$E_V(r)=\exp(-\int_0^r \rho s_D(y)G_V(y)dy)\ , \tag{3.18}$$

then it is clear that the elemental work $dW_V(r)$ required to expand a spherical cavity of radius r into a spherical cavity of radius $r+dr$ is

$$dW_V(r)=kT\rho s_D(r)G_V(r)dr\ . \tag{3.19}$$

From (2.14), (2.19), (2.20), and (3.18), we have for the cases $D=3$, 2, and 1, respectively,

$$G_V(x)=a+\frac{b}{x}+\frac{c}{x^2},\quad x>\tfrac{1}{2} \tag{3.20}$$

$$G_V(x)=\frac{1}{(1-\eta)^2}\left[1-\frac{\eta}{2x}\right],\quad x>\tfrac{1}{2} \tag{3.21}$$

$$G_V(x)=\frac{1}{1-\eta},\quad x>\tfrac{1}{2}\ , \tag{3.22}$$

where $x=r/2R$ is a dimensionless radius. Here a, b, and c are density-dependent constants given by (2.15)–(2.17), respectively. A combination of the expressions (3.20)–(3.22) into (3.19) and comparison to

$$dW_V(r)=pdv_D(r)+\sigma_0\left[1-\frac{2\delta}{r}\right]ds_D(r) \tag{3.23}$$

yields for $D=3$,

$$\sigma_0=\frac{-3\rho kT\eta(1+\eta)}{4(1-\eta)^3}\ , \tag{3.24}$$

$$\delta=\frac{\eta}{2(1+\eta)}\ ; \tag{3.25}$$

for $D=2$,

$$\sigma_0=-\frac{\eta}{2(1-\eta)^2}\rho kT\ , \tag{3.26}$$

$$\delta=0\ ; \tag{3.27}$$

and for $D=1$,

$$\sigma_0=\delta=0\ . \tag{3.28}$$

Note that the scaled-particle approximation predicts a nonzero value of δ for $D=3$, while for $D=2$ the parameter $\delta=0$, indicating that the contribution from curvature effects is negligible. The case of $D=1$ is degenerate in that there is no surface tension. Therefore, the work done due to surface change is given as

$$W_S(z,R)=\sigma_0\left[1-\frac{\delta}{R}\right]\Delta S\ , \tag{3.29}$$

where

$$\Delta S=\pi R^2 z\quad (D=3)\ , \tag{3.30}$$

$$\Delta S=2z\quad (D=2)\ , \tag{3.31}$$

$$\Delta S=0\quad (D=1)\ , \tag{3.32}$$

where σ_0 for $D=3$, 2, and 1 is given by (3.24), (3.26), and (3.28), respectively. The relations (3.6) and (3.29) yield the work necessary to expand the spherical cavity into a spherocylinder in terms of the dimensionless distance $x=z/2R$ as

$$W_2(x,R)=\frac{3\eta kT}{2(1-\eta)}x\quad (D=3)\ , \tag{3.33}$$

$$W_2(x,R)=\frac{4\eta kT}{\pi(1-\eta)}x\quad (D=2)\ , \tag{3.34}$$

$$W_2(x,R)=\frac{\eta kT}{(1-\eta)}x\quad (D=1)\ . \tag{3.35}$$

An alternative derivation of the expressions (3.33)–(3.35) for the work W_2 is given in Appendix B.

Finally, a combination of relations (3.4) and (3.33)–(3.35) yields the following analytical expressions for the lineal-path function for D-dimensional hard spheres in terms of the scaled distance $x=z/2R$,

$$L(x)=(1-\eta)\exp\left[-\frac{3\eta}{2(1-\eta)}x\right]\quad (D=3)\ , \tag{3.36}$$

$$L(x)=(1-\eta)\exp\left[-\frac{4\eta x}{\pi(1-\eta)}\right]\quad (D=2)\ , \tag{3.37}$$

$$L(x)=(1-\eta)\exp\left[-\frac{\eta x}{(1-\eta)}\right]\quad (D=1)\ . \tag{3.38}$$

In Figs. 4 and 5 we plot our analytical results for D-dimensional hard spheres at values of the sphere volume fraction $\phi_2=0.2$ and 0.5, respectively. For the case of $D=3$, we include our Monte Carlo calculations (see Ap-

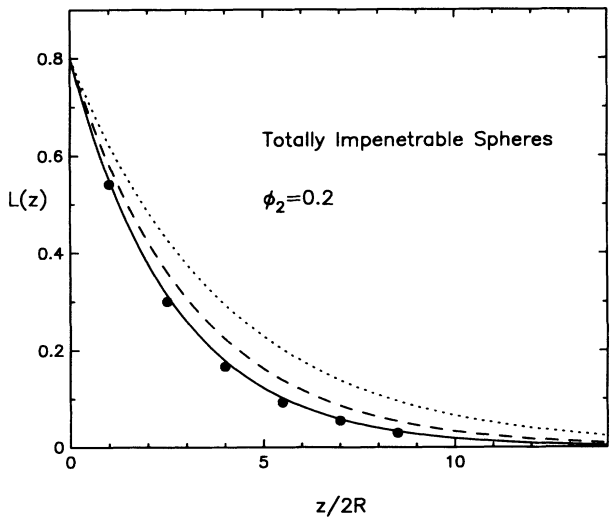

FIG. 4. Lineal-path function $L(z)$ vs the dimensionless distance $z/2R$ for D-dimensional totally impenetrable spheres at a sphere volume fraction $\phi_2=0.2$, as obtained from (3.33)–(3.35). The solid line is for $D=3$, the dashed line is for $D=2$, and the dotted line is for $D=1$. The solid circles are our Monte Carlo simulation results for $D=3$.

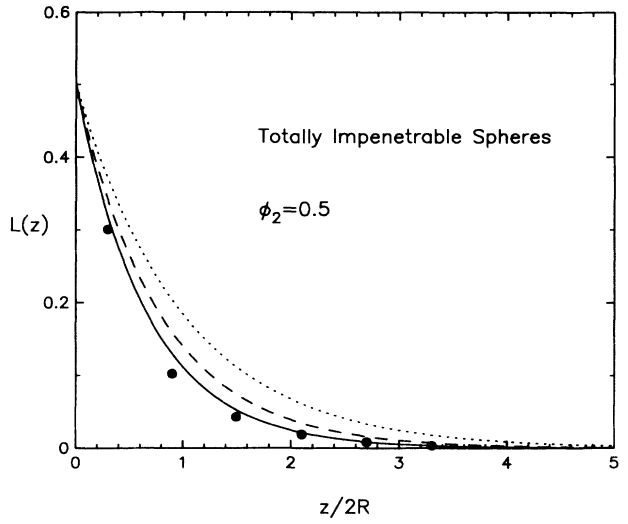

FIG. 5. Lineal-path function $L(z)$ vs the dimensionless distance $z/2R$ for D-dimensional totally impenetrable spheres at a sphere volume fraction $\phi_2=0.5$, as obtained from (3.33)–(3.35). The solid line is for $D=3$, the dashed line is for $D=2$, and the dotted line is for $D=1$. The solid circles are our Monte Carlo simulation results for $D=3$.

pendix A for details). In the case of $\phi_2=0.2$, our analytical results for $D=3$ agrees well with the simulation data. In the instance of $\phi_2=0.5$, our results for $D=3$ somewhat overestimate the data for intermediate z ($z\simeq 2R$) but gives better agreement for small and large z. Figure 6 compares the lineal-path function for fully penetrable spheres to the corresponding quantity for totally impenetrable spheres at $\phi_2=0.4$. The reason why the fully penetrable curve lies above the impenetrable curve is because the probability of finding void regions in the former system is larger than in the latter system [14].

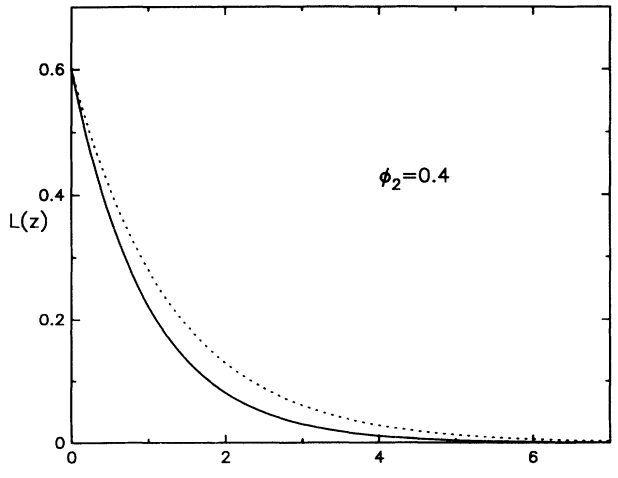

FIG. 6. The lineal-path function $L(z)$ for both fully penetrable and totally impenetrable three-dimensional spheres at a sphere volume fraction $\phi_2=0.4$, as obtained from (2.28) and (3.33), respectively. The solid line is for totally impenetrable spheres and the dotted line is for fully penetrable spheres.

IV. CONCLUSIONS

We have developed a systematic means of representing and computing the lineal-path function $L(z)$ for monodispersed system of D-dimensional spheres. In the case of fully penetrable spheres we obtained exact analytical expressions for $L(z)$ for any dimension. For totally impenetrable spheres, we found approximate but accurate expressions for $L(z)$ for arbitrary dimension. The accuracy of our method to obtain for $L(z)$ for hard-sphere systems depends upon the accuracy of the expression used for the conditional pair-distribution function G_V. Elsewhere we will generalize the present results to treat spheres with a polydispersivity of sizes. We have observed that the lineal-path function is identical to the area fraction of phase 1 measured from a projected image onto a plane, which is a quantity of fundamental interest in the fields of stereology and image science. In future work it will be shown [13] that the lineal-path function is directly related to other important morphological information of porous media, such as the chord-length distribution function [19] and the free-path distribution function associated with diffusion of gases in porous media [20].

ACKNOWLEDGMENT

This work was supported by the Office of Basic Energy Science, U.S. Department of Energy under Grant No. DE-FG05-86ER13482.

APPENDIX A: SIMULATION DETAILS

To test our theoretical results, Monte Carlo simulations are performed for three-dimensional systems of fully penetrable and totally impenetrable spheres. The simulation procedure consists of two basic steps: (i) generating equilibrium realizations of configurations of the particle systems, and (ii) sampling for the desired quantities.

For fully penetrable spheres, since there is no correlation between spheres, the distributions of the spheres are randomly and sequentially placed in a unit cell with periodic boundary conditions. For systems of totally impenetrable spheres, we employed a conventional Metropolis algorithm to generate equilibrium distributions of the particles. Spheres were initially placed in a cubical system on the sites of a regular lattice. Each sphere was moved by a randomly determined small distance to a new position, provided that no sphere overlap occurred. This process was repeated until equilibrium was achieved. To ensure that equilibrium was achieved, every sphere was moved 1500 times before we sampled. For every new realization, every sphere was then moved 20 times. Periodic boundary conditions were employed for systems of totally impenetrable sphere systems. Simulations for fully penetrable and totally impenetrable sphere systems were carried out with 10^5 and 800 particles, respectively.

The sampling procedure begins by randomly dropping line segments of length z_i ($i=1,2,3,\ldots$) in the system. The lengths of line segments were chosen to be $z_i=i\Delta z$ ($i=1,2,3,\ldots$) with $\Delta z=R/200$, where the radius of the spheres R is determined by the volume fraction of the spheres. When a line segment of length z_i is wholly in matrix phase, it is counted as a success. The probability $L(z)$ is then equal to the total number of successes divided by the total number of experiments. To get statistically reliable results, for every z_i, 2752 experiments were performed for every realization, and the probability $L(z)$ was obtained from a total of 100 realizations.

The case of fully penetrable spheres serves to test the accuracy of the simulation method since $L(z)$ is known exactly for this model [cf. (2.28)]. Figure 3 shows that the Monte Carlo calculations are in excellent agreement with the exact result (2.28). Monte Carlo results for hard spheres are depicted in Figs. 4 and 5 where they are compared to the approximate analytical result (3.33).

APPENDIX B: ALTERNATIVE DERIVATION OF THE EXPRESSIONS (3.33)–(3.35) FOR THE WORK $W_2(z,R)$

Here we provide an alternative means of deriving the relations (3.33)–(3.35) for the work $W_2(z,R)$ required to expand a spherical cavity of radius R into a spherocylinder of cylindrical length z and radius R, capped at each end by a hemisphere of radius R. As in the case of relation (3.19) for the work required to create a spherical cavity, we can write

$$W_2(z,R)=kT\pi R^2\int_0^z G_V(y=\tfrac{1}{2})dy\ , \tag{B1}$$

where $G_V(y=\frac{1}{2})$ is the conditional probability distribution associated with finding particle centers in contact with the spherical cap. This probability distribution is taken to be a constant since the radius of the hemisphere does not change as z changes. Employing the relations (3.20)–(3.22) for $G_V(y)$ with $y=R/2$, yields the expressions (3.33)–(3.35) for $W_2(x,R)$, where $x=z/2R$.

[1] S. Torquato, Appl. Mech. Rev. **44**, 37 (1991).

[2] G. W. Milton, Phys. Rev. Lett. **46**, 542 (1981); G. W. Milton, J. Appl. Phys. **52**, 5294 (1981); S. Torquato, *ibid.* **58**, 3790 (1985).

[3] G. W. Milton and N. Phan-Thien, Proc. R. Soc. London Ser. A **380**, 305 (1982).

[4] M. Doi, J. Phys. Soc. Jpn. **40**, 56 (1976).

[5] J. Rubinstein and S. Torquato, J. Chem. Phys. **88**, 6372 (1988); S. Torquato and J. Rubinstein, *ibid.* **90**, 1644 (1989).

[6] S. Prager, Phys. Fluids **4**, 1477 (1961); J. G. Berryman and G. W. Milton, J. Chem. Phys. **82**, 754 (1985).

[7] J. Rubinstein and S. Torquato, J. Fluid. Mech. **206**, 25 (1989).

[8] S. Torquato and M. Avellaneda, J. Chem. Phys. **65**, 6477 (1991).

[9] S. Torquato, J. Stat. Phys. **45**, 843 (1986); Phys. Rev. B **35**, 5385 (1987).

[10] B. Lu, and S. Torquato, Phys. Rev. A **43**, 2078 (1991).

[11] S. Torquato, J. D. Beasley, and Y. C. Chiew, J. Chem. Phys. **88**, 6540 (1988).

[12] E. E. Underwood, *Quantitative Stereology* (Addision-Wesley, Reading, MA, 1970).

[13] B. Lu and S. Torquato (unpublished).

[14] S. Torquato, B. Lu, and J. Rubinstein, Phys. Rev. A **41**, 2059 (1990); J. Phys. A **23**, L103-107 (1990). We would like to take this opportunity to correct some misprints in the above Physical Review A article: The second term of RHS of (5.6) should have a factor η^2; the argument of the exponential in Eq. (5.13) should be $-4\eta[(x^2-1)-\eta(x-1)]/(1-\eta)^2$; the plus sign in the argument of the exponential in Eq. (5.14) should be a minus sign; the x in the arguments of the exponentials of Eqs. (5.19) and (5.20) should be x^2. The RHS of Eq. (6.3) should be $[2\ln(1-\phi_2)^{-1}]^{-1}$; and the plus sign in Eq. (6.9) should be a minus sign.

[15] J. L. Lebowitz, Phys. Rev. A **133**, 895 (1964).

[16] H. Reiss, H. L. Frisch, and J. L. Lebowitz, J. Chem. Phys. **31**, 369 (1959).

[17] E. Hefland, H. L. Frisch, and J. L. Lebowitz, J. Chem. Phys. **34**, 1037 (1961).

[18] G. A. Mansoori, N. F. Carnahan, K. E. Starling, and T. W. Leland, J. Chem. Phys. **54**, 1523 (1971).

[19] A. H. Thompson, A. J. Katz, and C. E. Krohn, Adv. Phys. **36**, 625 (1987).

[20] T. K. Tokunaga, J. Chem. Phys. **82**, 5298 (1985).